An overview of the ITER electron cyclotron H&CD system

Massachusetts Institute of Technology

An Overview of the ITER Electron Cyclotron H&CD System

M. Henderson[a], F. Albajar[b], S. Alberti[c], U. Baruah[d], T. Bigelow[e], B. Becket[a], R. Bertizzolo[c], T. Bonicelli[b], A. Bruschi[f],
J. Caughman[e], R. Chavan[c], S. Cirant[f], A. Collazos[c], C. Darbos[a], M. deBaar[g], G. Denisov[h], D. Farina[f], F. Gandini[a], T. Gassman[a],
T.P. Goodman[c], R. Heidinger[b], J.P. Hogge[c], O. Jean[a], K. Kajiwara[i], W. Kasparek[j], S. Kasugai[i], S. Kern[l], N. Kobayashi[i],
J.D. Landis[c], A. Moro[f], C. Nazare[a], J. Oda[i], I. Paganakis[c], P. Platania[f], B. Plaum[j], E. Poli[k], L. Porte[c], B. Piosczyk[l], G. Ramponi[f],
S.L. Rao[d], D. Rasmussen[e], D. Ronden[g], G. Saibene[b], K. Sakamoto[i], F. Sanchez[c], T. Scherer[l], M. Shapiro[m], C. Sozzi[f], P. Spaeh[l],
D. Straus[l], O. Sauter[c], K. Takahashi[i], A. Tanga[a], R. Temkin[m], M. Thumm[l], M.Q. Tran[c], H. Zohm[k] and C. Zucca[c]

[a] ITER Organization, St. Paul-lez-Durance, 13067 France;
[b] Fusion for Energy, C/ Josep Pla 2, Torres Diagonal Litoral-B3,E-08019 Barcelona – Spain
[c] CRPP, Association EURATOM-Confédération Suisse, EPFL Ecublens, CH-1015 Lausanne, Suisse
[d] Institute for Plasma Research, Near Indira Bridge, Bhat, Gandhinagar, 382428, India
[e] US ITER Project Office, ORNL, 055 Commerce Park, PO Box 2008, Oak Ridge, TN 37831, USA
[f] Istituto di Fisica del Plasma, Association EURATOM-ENEA-CNR, Milano, Italy
[g] Association EURATOM-FOM, 3430 BE Nieuwegein, The Netherlands
[h] Institute of Applied Physics Russian Academy of Sciences, 46 Ulyanov Street, Nizhny Novgorod, 603950 Russia
[i] Japan Atomic Energy Agency (JAEA) 801-1 Mukoyama, Naka-shi, Ibaraki 311-0193 Japan
[j] Institut fur Plasmaforschung, Universitat Stuttgart, Pfaffenwaldring 31, D-70569 Stuttgart, Germany
[k]IPP-Garching, Association EURATOM-IPP,D-85748 Garching, Germany.
[l]Association EURATOM-FZK, IMF, Postfach3640 D-76021 Karlsruhe, Germany
[m] MIT Plasma Science and Fusion Center, Cambridge, MA 02139, USA

Abstract—**This Paper reviews the design and functionality of the 24MW 170GHz electron cyclotron heating and current drive system being planned for the ITER Tokamak. The sub-systems (power supplies, gyrotrons, transmission lines and launcher antennas) are described based on present day technologies, while on-going R&D provides component and sub-system testing with the possibility of increasing the reliability of the overall EC system. Modifications to the steering ranges of the launching antennas are under investigation that can improve the functional capabilities of the EC system without increasing cost and relaxing the engineering constraints.**

I. INTRODUCTION AND BACKGROUND

A 24MW CW Electron Cyclotron Heating and Current Drive (EC H&CD) system operating at 170GHz is to be installed for the ITER tokamak. The EC system will represent a large step forward in the use of microwave systems for plasma heating for fusion applications; present day systems are operating in relatively short pulses (≤10s) and installed power levels of ≤4.5MW. The magnitude of the ITER system necessitates a worldwide collaboration. This is also reflected in the EC system that is comprised of the power supplies, sources, transmission line and launchers. A partnership between Europe, India, Japan, Russia, United States and the ITER organization is formed to collaborate on design and R&D activities leading to the procurement, installation, commissioning and operation of this system.

The aim of this paper is to provide a brief review of the EC system design. In addition, the functional capabilities of the EC system are described followed by a summary.

II. TECHNICAL DESIGN

The ITER EC system (shown in figure 1) is comprised of four main sub-systems: 13 high voltage power supplies, 26 gyrotrons, the transmission lines and five launching antennas, and the additional ancillaries (control system, cooling, infrastructures, etc.). The functional requirements are to deliver ≥20MW at 170GHz for pulse lengths ≥800sec to the plasma for central heating, current drive and control some of the plasma instabilities.

The whole system is installed in three buildings as shown in figure 2. The power supplies (PS), gyrotrons and part of the transmission line (TL) are located in the RF building (top left building of figure 2). The TL pass through the Assembly hall building to the tokamak (bottom left), which houses the tokamak and the EC antennas (or launchers).

Figure 1: The ITER EC system comprised of power supplies, gyrotrons, transmission lines and launchers.
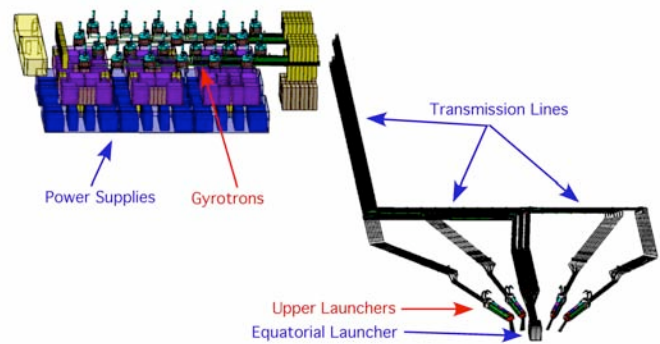
These subsystems are integrated together to provide a maximum operating flexibility and minimum downtime due to component failure by introducing a modular structure[1]. For example, a single power supplies powers only two gyrotrons to allow control of the delivered power in increments of 2MW. In the event of failure a single PS, gyrotron, TL or launcher can be isolated to allow continued operation of the remaining EC plant.

The power supplies consist of the main HVPS, body (BPS

and (for some gyrotrons) anode (APS) power supplies. The main HVPS provides the current (~90A) and roughly half the accelerating voltage (~55kV) of the electrons emitted from the gyrotron cathode. A pulse step modulated (PSM) concept is considered for the main HVPS, which provides high frequency modulation capabilities (≤5kHz) at competitive costs relative to thyristor systems[2]. The BPS provides the additional accelerating voltage (~45kV) in a depressed collector configuration to increase the electrical efficiency of the gyrotron to greater than 50%. A typical configuration of the power supplies and gyrotrons is shown in figure 3.

Figure 2: The EC system located in the three building: the power supplies and gyrotrons are located in the RF building (light green), the transmission line in all three building and the launchers in the tokamak building (light gray).
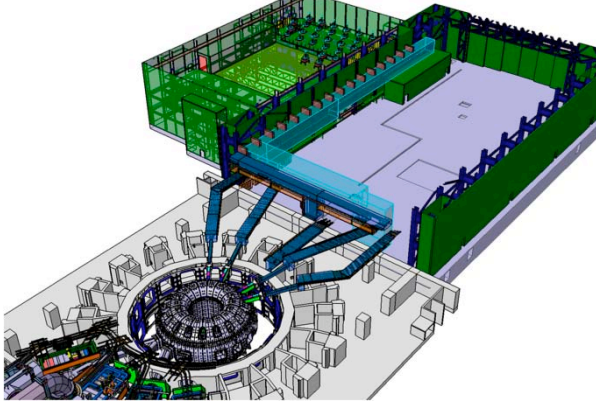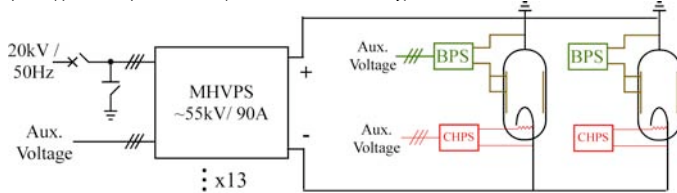

Figure 3: Typical configuration of the PS and gyrotrons[2], a single main high voltage PS powers two gyrotrons. Additional power supplies include the body (BPS), anode (not shown) and cathode heating PS.


The ITER in-kind procurement plans on the installation of three gyrotron types: a triode from Japan[3], a diode from Russia[4] and a 2MW co-axial from Europe[5]. India will also provide a single power supply and two gyrotrons (electing on one of the above types), which will be used as back-ups to the main 24MW system. All of the partners providing gyrotrons are performing prototype testing that aims at reliable demonstration of high power long pulse operation compatible with ITER specifications.

The gyrotrons are to have an electrical efficiency of >50% (coupled power to the waveguide divided by the applied input power) and a pulse length of ≥800sec (note that extension of the pulse length to 3'000 sec for long pulse operation is planned). The gyrotron output power is in a TEM_{00} mode that efficiently couples to the HE_{11} corrugated waveguide (63.5mm diameter), which forms the transmission line (TL). A matching optics unit (MOU) is inserted between the gyrotron and HE_{11} waveguide to reshape and orientate the beam for optimum coupling into the TL. An additional switch connected to a load is installed in the transmission line for gyrotron installation and conditioning.

The TL[6] guides the RF power from the gyotron over a distance of ~160m to the launchers. In addition, the TL monitors the gyrotron output power, modifies the polarization for optimum plasma coupling and directs the power to either an equatorial or one of four upper launchers installed in the ITER ports via an in line switching system. Figure 4 illustrates the components that form a typical TL and provide the above functionality. Note that an additional switch is introduced in each line to deviate the power to a calorimetric load for gyrotron conditioning.

The routing of the TL through the three buildings was chosen to minimize the number of mitre bends, which are the greatest sources of transmission losses. The total number of mitre bends have been reduced from between 9 to 12 down to 7 to 9 depending on the path to the EL or UL. The estimated transmission efficiency is ~90to 92%, comparable to the ~95% transmission efficiency measured in the JAEA 7 mitre bend test stand[7].

Figure 4: The primary components forming a typical transmission line, which is used to transmit the EC power from the gyrotrons to the launchers.
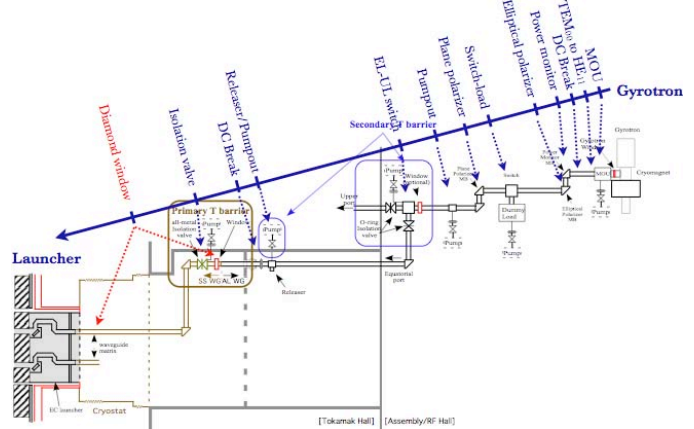
Diamond windows[8] are placed at the entry of both the EL and UL, which create a vacuum and tritium barrier between the launchers and TL. The window prevents tritium from traveling from the launcher (at torus pressure) up the waveguide to the gyrotrons (note that the TL is also evacuated). All-metal valves are placed near the windows to provide a hard barrier in the event the diamond window fails.

Figure 5: The Equatorial Launcher (EL)[9] steers up to 24 beams across the central half of the plasma cross section. The three steering mirrors provide toroidal steering for maximizing the driven current for central heating and current drive applications.
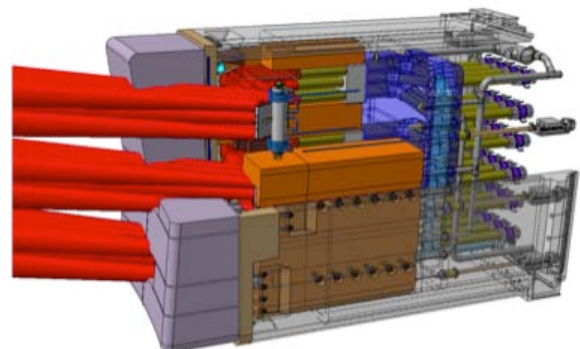

There are two types of launchers used to inject the EC

power into the plasma: one equatorial (EL) and four upper (UL) launchers. The EL[9] has a total of 24 waveguide entries that are divided into sets of 8 beams on to three steering mirrors as shown in figure 5. The beams are steered in the toroidal (or horizontal) section, which provides access from on axis to near mid radius and maximizes the driven current.

The four UL[10] ports each have 8 entries that are split in two sets of 4 beams as shown in figure 6. There are three fixed and one steering mirror for each beam set, these mirrors are used to focus and assemble the four beams such that the deposited power forms a peaked current density profile, optimum for the control of magneto-hydrodynamic (MHD) instabilities[11-12], in particular the neoclassical tearing modes (NTMs) that can degrade the fusion performance by up to 50%. The NTMs are expected to occur on the q=3/2 and 2 flux surfaces for the plasma scenarios 2, 3a and 5 in the range of ~$0.55 \leq \rho_T \leq$~0.85, where ρ_T is the square root of the normalized toroidal flux.

Figure 6: The Upper Launcher (UL) [10] steers up to 8 beams across the outer half of the plasma cross section. Four mirrors are used to reconfigure and focus the beams for a small deposition profile ideal for the control of MHD activity.
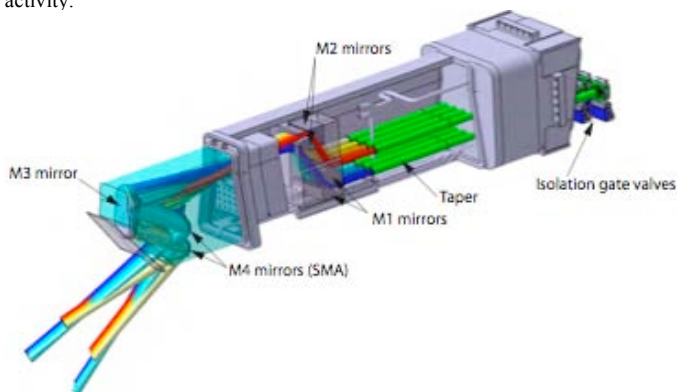
Between the EL and UL, there are a total of 11 steerable mirrors to allow a large flexibility in using the EC power for multiple applications simultaneously. A remote controllable switch (switching speed of ≤ 2 sec) is in included in each TL that redirects the EC power to either EL or UL.

The control of the EC deposition location will be performed by an active feed back control system that monitors the deposition location relative to the target position and redirects the location as necessary. In addition the control system will calculate the desired polarization, then set the polarizers (located in the transmission line) for optimum plasma coupling.

The vast majority of the components to be used to form the ITER EC system have never been used on an existing experimental fusion device. For this reason, many of the components are undergoing prototype testing followed by design improvements to ensure compatibility with the ITER requirements. In addition, as new technologies offer improved components, these will be tested at ITER compatible power and pulse lengths. If successful, the ITER EC system design will be modified to include these new technologies that offer improved transmission efficiency, increased functionality or cost reduction.

III. FUNCTIONAL CAPABILITIES

The functional capabilities of the EC system strongly depend on the focusing and access range provided by the two launchers. The original baseline design (prior to 2007) partitioned the physics applications between the two launchers based on regions in the plasma. The EL accessing inside of $\rho_T \leq$~0.55 for applications associated with central heating, current drive and sawtooth control. The UL accesses the region where NTMs are expected to occur between ~$0.55 \leq \rho_T \leq$~0.85. This partitioning had some short comings: the EL had to cover twice the steering region as the UL and the EL had to be designed for both central heating applications (preference toward a broad deposition profile) and control of the sawtooth applications (preference toward a narrow deposition profile). An EL design compatible with providing both a broad and narrow deposition profile over the prescribed steering range was not feasible. The large demands on the EL resulted in limited performance and access range, not achieving the desired accessibility over ~$0.0 \leq \rho_T \leq$~0.55. A large beam shine through occurred at toroidal injection angles larger than 41°, which prevented access of ~$0.45 \leq \rho_T \leq$~0.55 (dashed blue curve of figure 7) [13].

Figure 7: The accessibility of the combined EL and UL is illustrated as the maximum power that can be deposited at any given location. The blue dashed line corresponds to the baseline configuration and the green line to the proposed re-partitioning of the physics applications between the UL and EL[13-14].
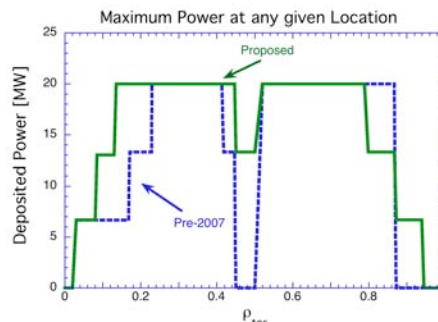
An alternative partitioning of the physics applications has been proposed[13-14] that divides the functional requirements based on the need for broad or narrow deposition profiles. The EL would still be used for central heating and current drive applications, but the UL would be used for the control of both the NTM and sawtooth instabilities. The UL is modified to access the sawtooth by spreading out the access region of the upper and lower steering mirrors as shown in figure 8.

The upper steering mirror is aimed more centrally to access inside ρ_T~0.3, while the lower steering mirror accesses the outer flux surfaces. An overlap region between ~$0.55 \leq \rho_T \leq$~0.80 is accessible to either the upper or lower steering mirrors. The overall steering angle of the mirror is reduced to relax the engineering constraints and improve the longevity of the steering mechanism. The improved access is illustrated by the solid green curve of figure 7.

Note that the EL baseline design has all the beams steered in a horizontal plane. The top and bottom beam sets miss the plasma center as shown in figure 9 (left side). A poloidal tilt of

±5° can be introduced to provide more central access as illustrated in figure 9 (right side). This modification would increase the coverage of the top and bottom steering mirrors.

Figure 8: The increased UL access range is achieved by spreading the steering range of the upper (USM) and lower (LSM) steering mirrors, with the USM aiming further inward.
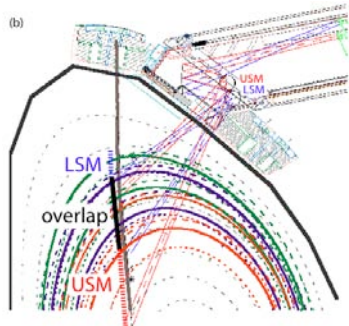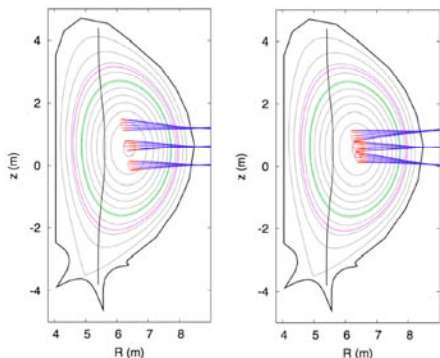

Figure 9: The limited central access of the EL (left figure) is improved by introducing a small poloidal tilt in the top and bottom steering rows (right figure).

The EL and UL beams are all aimed to provide co current drive (current driven co-linear with the plasma current). An additional proposal is to flip one steering row of the EL to inject 8MW of power in the counter direction (driving current in the opposite direction of the plasma current). This would provide sufficient flexibility to either drive 20MW in the co-direction (by balancing 16MW in the EL and 8MW in the UL-USM) or zero net current (8MW counter from the EL and 16MW in the UL-USM). Note that the EL drives roughly twice the current as the UL.

This additional flexibility decouples the heating from the current drive functions. For example, pure on axis heating is useful for impurity control while avoids peaking of the central plasma current. The counter current drive can also be used to tailor the plasma current profile to either maintain a flat central shear for avoiding sawteeth or introducing a hollow profile for generating and sustaining an internal transport barrier, as illustrated in figure 10.

IV. SUMMARY

The 24MW EC system designed for ITER is progressing in design detail, aiming for improved functionality while attempting to minimize the operational risks and when possible costs. The system is being advanced by an international team that is involved in the design and procurement of the system, which includes 13 power supply

sets, 26 gyrotrons, the associated transmission lines and five launching antennas. Prototype testing of the systems is in progress to evaluate their performance and propose alternative designs for improved reliability.

Figure 10: Introducing 8MW of counter current drive provides a large capability in tailoring the current profile by adjusting the on and off-axis driven current in the co and counter directions as shown for the q-profile of scenario 4[15].
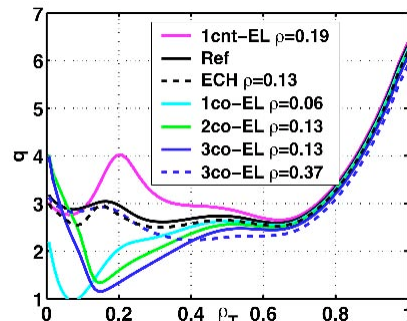
In addition, an alternative partitioning of the EC launchers accessibility is being investigated, which offers increased accessibility of the EC power nearly throughout the plasma cross sections. The proposal would relax the EL launcher functionality (remove the access $\rho_T>0.45$) and modify the steering angles for improved central access and counter current drive injection for decoupling the heating and current drive functionality. The UL is modified to include access into $\rho_T\leq\sim0.3$ for the control of the sawtooth. These modifications would increase the capabilities, while reducing the engineering constraints on the EC system.

REFERENCES

[1] M. Henderson and G. Saibene, Nucl. Fusion **48** (2008) 054017.
[2] D. Fasel *et al*, *Fusion Sci. Technol.* **53** (2008) 246.
[3] K. Sakamoto *et al Nature* **3** (2007) 411–4.
[4] G. Denisov *et al* Development in Russia of high power gyrotrons for fusion *Proc. 4th IAEA ECRH Technical Meeting (Vienna, Austria, May 2007).*
[5] J.-P. Hogge *et al J. Phys. Conf. Ser.* **25** (2005) 33.
[6] D. Rasmussen *et al* Design of the ITER electron heating *and current drive waveguide transmission line Proc. 4th* IAEA ECRH Technical Meeting (Vienna, Austria, May 2007).
[7] Takahashi K. *et al, 8th IEEE Int. Vacuum Electronics Conference, (Kitakyushi, Japan, May 2007).*
[8] R. Heidinger et al., Fusion Eng. Des. **82** (2007) 693.
[9] Takahashi K. *et al* Nucl. Fusion **48** (2008) 054014.
[10] M. Henderson et al Nucl. Fusion **48** (2008) 054013.
[11] S. Gunter *et al Phys. Rev. Lett.* **87** (2001) 275001.
[12] C. Angioni *et al Nucl. Fusion* **43** (2003) 455.
[13] G. Ramponi et al, Nucl. Fusion **48** (2008) 054012.
[14] M. Henderson et al, *et al* 2006 *Proc. 21st Int. Conf. on Fusion Energy 2006 (Chengdu, China, 2006)* IT/P2-15.
[15] C. Zucca et al, Theory of Fusion Plasmas AIP Conf. Proc. **1069** (2008) 361.